Vol. 47, No. 3 (2025) 498-512, DOI: 10.24874/ti.1952.05.25.07

Tribology in Industry

www.tribology.rs

RESEARCH

Friction and Abrasive Wear Behavior of FDM Printed PLA Structures

Maximiliano Zanin[a,b,*], Pablo Rojas[a], Nicolás Urbano Pintos[a], Vitaly Martynenko[a,c], Alejo Nahue Angiano[a]

[a]Universidad Tecnológica Nacional, Facultad Regional Haedo, Laboratorio de Ensayos de Desgaste y Fricción Sólida (LEDFS), Haedo, Buenos Aires, Argentina,
[b]Instituto de Investigaciones Científicas y Técnicas para la Defensa (CITEDEF), Villa Martelli, Buenos Aires, Argentina,
[c]Centro de Investigación y Desarrollo en Mecánica, Instituto Nacional de Tecnología Industrial (INTI), Miguelete, Buenos Aires, Argentina.

Keywords:

3D printing
Polylactic acid
FDM
Friction
Abrasive wear
Infill pattern
Infill density

* Corresponding author:

Maximiliano Zanin
E-mail: mzanin@frh.utn.edu.ar

Received: 21 May 2025
Revised: 20 June 2025
Accepted: 28 July 2025

A B S T R A C T

In rapid prototyping industries - such as aerospace and biomedical engineering - 3D printed polylactic acid (PLA) models used in investment casting require high-quality surface finishes to prevent the transfer of printing defects to the final metal components. Among various post-processing methods, sanding is widely used due to its low cost, ease of control, and ability to reduce surface roughness. This study investigates the abrasive wear and friction behavior of PLA specimens with three infill patterns (linear, triangular, trihexagonal) and three infill densities (50%, 75%, 100%) tested against abrasive papers of four grit sizes (60, 150, 320, 600) under Pin-on-Disc conditions (0.033 m/s, 40 N, 1800 s). The lowest and most stable CoF (~0.55) was recorded with 320-grit paper. Wear rates decreased with increasing infill density for grits 150, 320, and 600, reaching a 50% reduction at 100% density. In contrast, 60-grit tests showed increased wear at higher densities. Surface analysis revealed micro ploughing, and polymeric burr formation. Finer abrasives promoted debris agglomeration on the pin, creating clean "drag bands" on the abrasive disc. These results offer design insights for optimizing 3D printing process parameters to enhance tribological performance in PLA-based components subjected to surface finishing or abrasive contact.

1. INTRODUCTION

Strict environmental regulations and increasing environmental awareness in the industry in recent years have driven the search for sustainable alternative materials with improved mechanical and tribological properties [1,2]. Recent studies propose polylactic acid (PLA) as one of the biodegradable alternatives to replace conventional polymers in cost-effective engineering applications. This polymer is widely used in fused deposition modeling (FDM) due to its low cost and ease of processing. These alternative materials, combined with recent advances in 3D printing techniques, offer an economically viable approach, simultaneously reducing energy consumption and promoting sustainable technologies [3,4]. These qualities, reduced manufacturing times and complex geometries, make it suitable to produce casting models like lost-wax models [5,6].

The capability of FDM to fabricate parts with virtually any geometry necessitates a comprehensive understanding not only of material properties but also of the influence of different infill architectures and densities on mechanical performance [7]. According to the literature, research on tensile properties has been prioritized over tribological characteristics, with less than 5% of total mechanical characterizations focusing on tribological studies [8]. The mechanical properties of FDM-printed parts are strongly influenced by geometric design parameters such as build orientation, layer thickness, infill density, and infill pattern. Several studies have shown that tensile strength and elastic modulus tend to increase with infill density, regardless of the infill pattern [9]. Conversely, other authors have reported that mechanical performance may depend primarily on the selected infill architecture. Patterns such as honeycomb, grid, and triangular have demonstrated favorable mechanical behavior, though not necessarily at maximum infill density [10-13]. Various studies have shown that infill density and pattern influence the tribological behavior of polymeric 3D-printed components.

Print orientation, layer height, density and infill pattern are just some of the variables studied in different tribological behaviors for 3D printed structures [14-19]. Several studies have reported on PoD tests conducted on FDM-printed PLA specimens to assess the effect of printing parameters on tribological performance. Renganathan investigated three different infill patterns—concentric, linear, and Hilbert—at two printing speeds, finding that the Hilbert pattern revealed the lowest CoF compared to concentric and linear patterns [20]. Aziz et al. analyzed the friction behavior of samples with circular surface textures of varying diameters, identifying an optimal texture that minimized CoF at both high and low sliding speeds in dry contact. Additionally, they found that lower infill densities, which correspond to larger voids in the texture, exhibited reduced entrapment of wear debris. However, when the surface texture featured larger voids, CoF increased due to the reduced real contact area [21]. Portoacă et al. evaluated the tribological performance of PLA-on-PLA samples in PoD tests. Their study involved specimens printed in an X-Y build model with a 45° orientation, varying infill densities (50%, 75%, and 100%) and layer thicknesses (0.1, 0.15, and 0.2 mm). They reported that the lowest CoF and wear rates were achieved with the largest layer thickness, while the optimal infill percentages for minimizing wear and friction were 75% and 50%, respectively [22]. For PLA samples with diamond-shaped infill, the lowest wear was observed at a printing speed of 45±5 mm/s and a temperature of 190°C [23]. Ramadan et al. compared the tribological performance of PLA, ABS, PCL, and co-polyester in 100% triangular infill structures using PoD tests against low-roughness steel disks (Ra = 0.023 μm). Their findings indicated that wear was inversely proportional to the hardness of the printed structures, while friction behavior was inversely proportional to the average linear roughness of the pins. Among the investigated polymers, PLA exhibited the lowest CoF and wear rates [24]. Other studies have reported no significant influence of print orientation on tribological behavior in PoD tests conducted under high loads and extended test durations [25]. Istif evaluated horizontally and vertically printed PLA pins with a 100% linear infill pattern against steel and cast-iron disks with varying roughness. The lowest wear rates were reported for higher surface roughness conditions, whereas no significant difference in friction behavior was observed between the two build orientations [26]. Pawlak et al. studied neat PLA structures and PLA reinforced with MoS_2 against steel disks with a roughness of Ra = 0.4 ± 0.05 μm in prolonged testing (9000 s) under low loads. For pure PLA samples, the lowest friction force was reported at the end of the test compared to PLA-MoS_2 composites [27].

Moreover, traditional wax-based investment casting models are increasingly being replaced by 3D-printed PLA patterns due to their significantly reduced fabrication time and cost. However, the advantages of producing these models using FDM techniques are offset by drawbacks such as the stepped surface finish, internal porosity, infill patterns, and other print-related features that can negatively impact the surface roughness and dimensional tolerances of the final cast components. Surface finishing strategies have been explored in prior research, including medical implant prototypes by Tiwary et al. [28], mechanical part patterns by Ol'khovik [29], and abrasion resistance comparisons between extruded and 3D-printed PLA by Kujawa & Ptak [30]. Manual sanding or surface smoothing using handheld rotary tools remains one of the most economical, user-friendly, and controllable methods for improving the surface finish of PLA patterns used in lost-PLA casting processes. Although abrasive wear of polymers has been studied for decades through Pin-on-Disk (PoD) tests [31-35], limited data exist on the abrasive wear behavior of PLA-based FDM structures. To date, no comprehensive study has evaluated the combined influence of multiple infill patterns, densities, and abrasive grades in a single experimental framework.

Given that triangular, trihexagonal, and honeycomb-like infill architectures exhibit enhanced directional stiffness and near-isotropic mechanical behavior [10-13], and considering the lack of systematic studies involving abrasive wear without abrasive renewal, to address this gap, the present study undertakes a comprehensive PoD investigation on FDM-printed PLA specimens, with the following contributions: (1) comparative analysis of three infill patterns, Linear (L), Trihexagonal (TH), and Triangular (T); (2) evaluation of three infill densities (50%, 75%, and 100%); (3) assessment of four abrasive grit sizes (60, 150, 320, and 600); and (4) correlation of wear rates and friction coefficients with both print parameter and abrasive severity. The findings provide practical insights for the design and optimization of 3D-printed PLA components intended for environments involving severe abrasive contact.

2. MATERIALS AND METHODS

2.1 Materials and preparation

In this study, cylindrical pin specimens were fabricated with a height of 10 mm and a diameter of 10 mm, featuring a support section of 10 mm in length and 5 mm in diameter. The pins were printed via FDM using a 1.75 mm PLA filament (Grilon3, Argentina). This material has properties poorly defined by the manufacturer (Table 1).

Table 1. PLA properties according to manufacturer.

Property	Value
Density	1.24 g/cm^3
Melting temperature	145-160 °C
Glass transition temperature	55-60 °C
Tensile strength	55-72 MPa
Tensile elongation	6 %
Young's modulus	3.6 MPa

The 3D printing process was carried out via Fused Deposition Modeling (FDM) using a Hellbot MAGNA-SE 32-bit (Argentina) printer. The cylindrical samples were printed with three different infill patterns (Linear, Trihexagonal, and Triangular), as illustrated in Figure 1, each with three distinct infill densities (50%, 75%, and 100%).

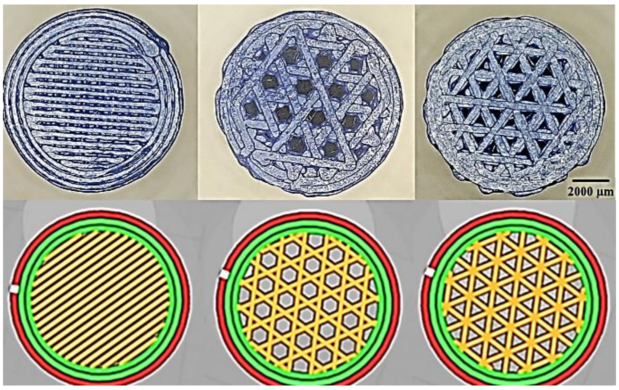

Fig. 1. Top view comparison of polymer pin surfaces with 50% infill density (top row) and their corresponding infill pattern designs (bottom row).

The printing parameters were consistent for all pin constructions, as detailed in Table 2. The printing temperature and speed were chosen following the recommendations of Renganathan [20] and Portoacă et al. [22].

Table 2. The 3D-printing parameters.

Parameter	Value
Nozzle diameter	0.40 mm
Extruder temperature	190°C
Platform temperature	60°C
Layer Thickness	0.20 mm
Filament diameter	1.75 mm
Wall thickness	0.80 mm
Print speed	60 mm/s
Material/ Filament Colour	PLA / Blue
Infill density	50%,75%, 100%
Build pattern	L, T and TH

A printing temperature of 190°C was adopted based on the findings of Zainal et al. [36], aiming to achieve the lowest coefficient of friction, although these authors reported a high wear rate in low-density structures. Conversely, Yaman et al. [37] observed good wear resistance in structures with 100% infill at 190°C. The layer height was selected based on studies reporting improved tensile and wear resistance [22,38].

2.2. Tribological testing

Tribological properties were evaluated using a Pin-on-Disc tribometer developed at the Wear and Solid Friction Testing Laboratory of the National Technological University – Haedo Regional Faculty. Tests were carried out under dry sliding conditions, following the ASTM G99-17 standard [39] (see Fig. 2), using a rotation speed of 20 rpm (0.033 m/s) and a normal load of 40 N. Low loads and speeds less than 0.5 m/s were selected to prevent heat-induced softening and surface deformation during testing as indicated by [20-22, 40]. The total test duration was set to 1800 seconds, corresponding to a sliding distance of 59.4 m.

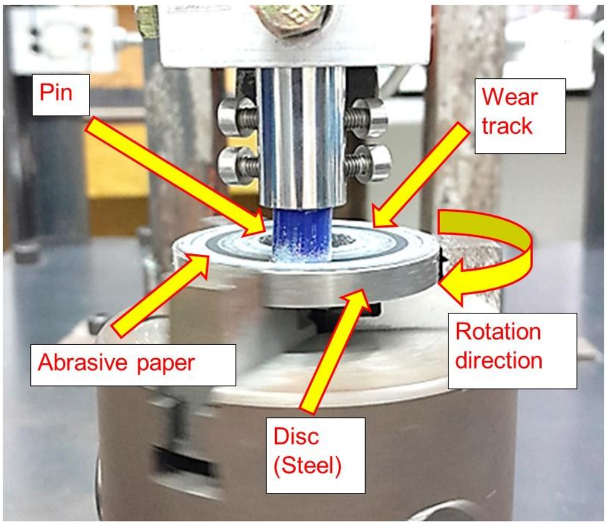

Fig. 2. Abrasive wear of pin samples against SiC abrasive paper bonded disc steel.

For pre-test preparation, it was ensured that the pins were positioned perpendicular to the rotating abrasive paper on the steel disc to reduce unwanted errors and ensure repeatability [41]. For the tests, three or more samples were examined for each combination of pattern and fill density with each abrasive. Abrasion tests were performed under ambient conditions (25 ± 2 °C and 50±10 RH). The friction behavior was recorded during the entire time of each test (1800s). The samples were weighed before and after each test using a RADWAG - AS220 (Poland) balance with a scale resolution value of 0.0001 g to determine mass loss ΔP (g). The morphologies of the worn-out surfaces of the polymeric samples and surfaces of the abrasive discs were evaluated using optical microscopy techniques and digital processing. Microscopic observation was performed using a MOTIC BA310MET (China) optical microscope and a CELESTRON 44308 (USA) 20×, 5 MPx digital microscope. Some studies suggest that colored filaments exhibit enhanced mechanical properties and surface finish [38,42,43]. The filament color was chosen to facilitate optical microscopy observations and digital image processing. Commercial aluminum oxide (Al_2O_3) abrasive papers (DobleA-AX51/AX52, Argentina) with grit sizes of 60, 150, 320 and 600 were used. Each abrasive paper was bonded to a 50 mm-diameter steel disc using high-adhesion double-sided tape, creating a wear track with an average diameter of 31.5 mm. The friction surfaces were thoroughly cleaned with isopropyl alcohol in an ultrasonic bath for 600 s to remove loose particles. They were then allowed to dry at room temperature before being weighed and examined microscopically.

Test sets were named by infill pattern/infill density/grit of the abrasive paper. For example, when L/75/320 is indicated, it indicates the results of tests performed with a Linear pattern, 75% infill densities against 320-grit abrasive paper. When a number or letter is left out it refers to all tests with the indicated characteristics. For example, TH/--/150 indicates the test set with a Trihexagonal infill pattern against the 150-grit abrasive paper regardless of infill density.

3. RESULTS AND DISCUSSION

3.1 Friction behavior

Based on the results obtained, the friction behavior is presented and discussed, highlighting the abrasive counterpart as the dominant factor. Likewise, the influences of the different filling patterns and densities of the 3D-printed PLA samples are analyzed. All reported coefficients of friction represent the mean of at least three independent tests conducted under identical specimen and counterpart conditions.

The coefficient of friction curves can show three stages (see Fig. 3 and 4). Stage 1: rise of the CoF to a maximum (running-in). Stage 2: fluctuating friction and/or continuous decrease of the CoF, and Stage 3: stable friction. Stage 1 was characterized by a sudden transition from a static state to a sliding motion. This initial stage can show growth until the next stage, or it can also raise the CoF to a certain peak and then descend to a more stable behavior. Stage 2 is an intermediate transition between the running-in and the stable period. It was characterized by a fluctuating behavior to a greater or lesser extent until attenuating (see Fig. 4) or by a decrease of the maximum peak characteristic of stage 1. In some cases, this transition stage can be characterized by a fluctuating decrease (See Fig. 3). Stage 3 shows a process of constant friction with few fluctuations where the most stable behavior is presented. Some stages may not manifest [17,44].

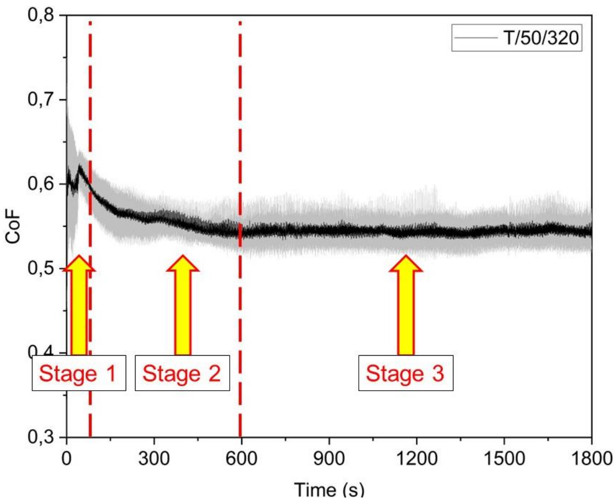

Fig. 3. Characteristic stages of friction behavior as against sliding time (T/50/320 tests).

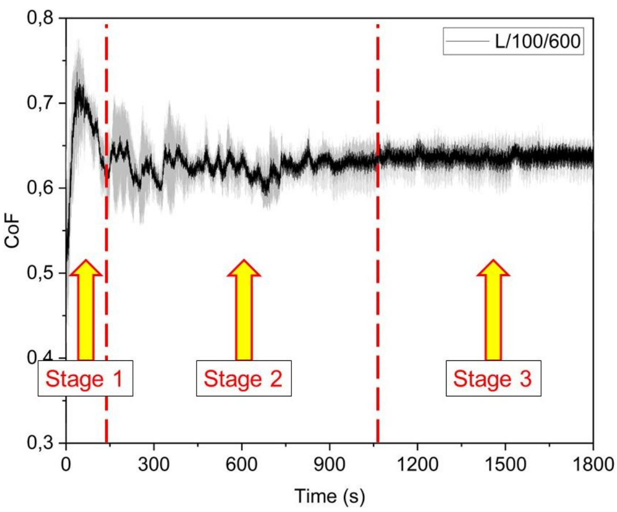

Fig. 4. Characteristic stages of friction behavior as against sliding time (L/100/600 tests).

Regardless of the filler pattern, all tests with 60-grit abrasive paper (--/--/60) showed similar friction behavior, with a continuing decrease in CoF. The friction behavior with this abrasive resembles that of Stage 2, with a wide range of results but no stable CoF (See Fig. 5). The reduction in CoF occurs more rapidly in samples with lower infill density. Open structures likely retain a greater number of particles. Furthermore, as will be detailed later, polymer burrs form, softening the contact interface. These factors together promote a continuous reduction in CoF.

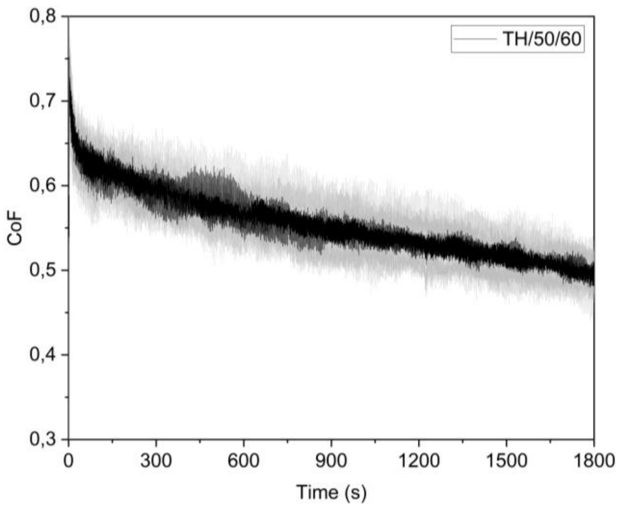

Fig. 5. Typical friction behavior of tests on 60-grit sandpaper (TH-50-60).

The progressive decline in the coefficient of friction (CoF) can be attributed to two interrelated mechanisms: (1) the mitigation of particle jamming at the sliding interface, and (2) a wear debris generation rate that exceeds its removal. This imbalance promotes the formation and accumulation of a persistent third-body layer at the interface, which prevents the CoF from stabilizing into a steady-state plateau. Notably, specimens with triangular (T) and trihexagonal (TH) infill patterns exhibited slightly greater reductions in CoF compared to those with a linear pattern, suggesting that internal geometry poor influences debris retention and overall frictional behavior.

In tests with 60-grit sandpaper, the varying orientations of the T and TH patterns likely lead to differences in particle size and agglomeration at the contact interface. Different particle sizes contribute to the decrease in COF. The sharpest declines in CoF were observed with the T and TH patterns, starting at 0.68 and decreasing to 0.5 toward the end of the test (see Fig. 5). It was not possible to obtain an average COF with 60-grit sandpaper because the friction behavior did not present a stable period throughout the test. However, the average CoF values analyzed in at the end of each test range between 0.59 ± 0.09. These values correlate with those expressed by Ertane et al. in reciprocating tests at low loads [45]. The CoF values are like those reported by Palaniandy et al. in PoD tests on steel [40].

Figure 6 presents a comparison of three typical friction behaviors over sliding time for linear patterns with infill densities of (a) 50%, (b) 75%, and (c) 100%. As the material density in contact with the abrasive increases, polymer fragments tend to detach more easily and rapidly fill the valleys between the abrasive asperities. These fine particles are likely to remain within the wear track and accumulate at the sliding interface, promoting the early formation of a transfer film. The presence of this transfer film helps stabilize the friction behavior, resulting in a uniform CoF trend (Stage 3). The thickness of the transfer layer and the morphology of the debris play key roles in establishing tribological stability [46]. Additionally, the amplitude of the recorded CoF signals is lower than that observed with the 60-grit abrasive paper.

The friction behavior observed for the 150-grit tests with 50% infill density was characterized by a gradual decline in CoF (see Fig. 6a), although with a gentler slope compared to the 60-grit results (see Fig. 5). No significant differences were detected among the different infill patterns under this abrasive condition. As the infill density increases, the CoF tends to stabilize more rapidly, reaching a well-defined plateau at 100% infill density. This progressive stabilization is observable from Fig. 6a through Fig. 6c.

Tests with 320-grit abrasive paper produce the most stable friction behaviors and the least data dispersion. With increased filler density, stages 1 and 2 are reduced by 66%, resulting in a stable CoF. Figure 7 show typical friction behaviors obtained from tests on 320-grit sandpaper samples with triangular and trihexagonal patterns. Tests on 320-grit abrasive paper showed the highest stability and lowest CoF.

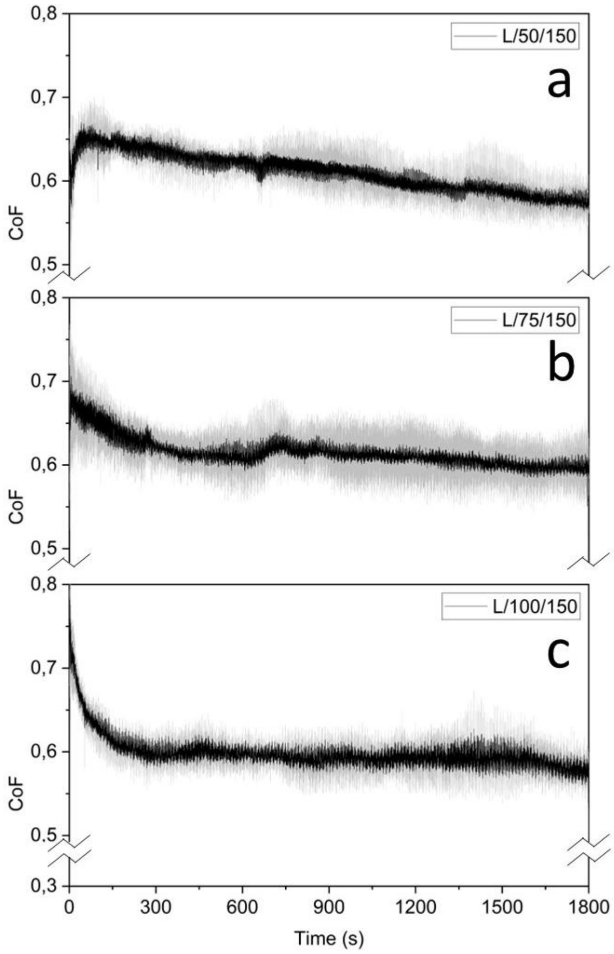

Fig. 6. Comparative friction behavior of PLA pins with different infill densities (a: 50%, b: 75%, c: 100%) tested on 150-grit abrasive paper. The figure is presented as a composite panel to allow direct visual comparison of friction trends.

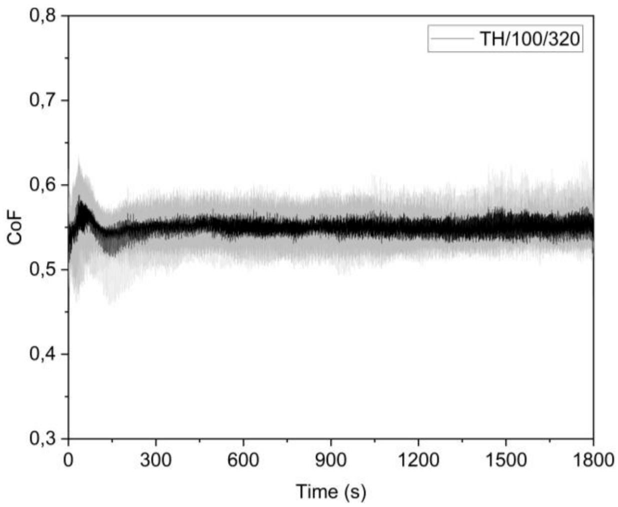

Fig. 7. Typical friction behavior of tests on 320-grit sandpaper (T/100/320).

Tests on 600 grit abrasive paper revealed non-periodic irregularities in friction behavior (Stage 2) for up to 1000 ± 100 s. Figure 4 shows a typical image of friction behavior on 600-grit paper. The non-periodic irregularities in Stage 2 could be attributed to the discontinuous formation of the transfer film and transfer of agglomerated material to the pin, as detailed in the analysis of the wear surfaces. Furthermore, a well-defined Stage 3 is identified, with a consistent average COF slightly higher than that obtained with 320-grit paper. Only samples built with linear patterns show a reduction in Stages 1 and 2 as filling density increases. The friction behavior showed no significant differences in the filling pattern. However, some authors suggest that larger spaces in the surface texture can result in a slight increase in CoF, as the friction force is proportional to the actual contact area [21]. Zhiani et al. found comparable CoF values in PoD tests with concentric print patterns but at higher speeds [25]. Other researchers believe that an appropriate filling pattern can reduce the trapping of detached particles, preventing the formation of a transfer film that raises the CoF [21]. Infill density is more relevant than infill-pattern in analyzing friction behavior. Compared to 60-grit sandpaper, the slope of the friction coefficient decreases as the filler density increases. In addition, a reduction in abrasive grain size and increased infill density stabilizes and shorten stages 1 and 2. The counterpart roughness has a substantial effect on friction behavior. The average CoF decreases with decreasing abrasive grain size up to 320-grit, except for 600-grit, which increases slightly again. Zainal et al. reported an increase in CoF as counterpart roughness increased [36], whereas Istif reported that CoF did not change with roughness variations [26]. The 320-grit sandpaper shows the lowest average CoF with a small standard deviation (stage 3).

The spaces and valleys between the abrasive asperities decrease as the abrasive grain size decreases. During sliding, the abrasive's smaller valleys allow for premature filling, causing the transferred material to stay longer.

First, the material transferred to the abrasive surface causes surfaces to become less rough as sliding proceeds (Stages 1 and 2). Second, the transferred material is trapped in the rough surface's valleys. The friction behavior is stabilized (Stage 3) by the transferred material acting as a lubricant between the sliding surfaces [47]. The contact area grows as the counterpart's roughness reduces, which lowers pressure and, in turn, CoF [17].
As the rubbing distance increases, frictional heat can cause softening that allows valley filling [25]. One factor that reduced the coefficient of friction was the formation of thin, segmented polymer films. When 600-grit sandpaper was used as a counterpart, a mixture of small abrasive particles and polymer debris was observed on the pins. The mixed polymer debris and fine abrasive particles caused fluctuations in the friction behavior until it stabilized.

3.2 Wear behavior

Wear was evaluated in terms of mass loss, showing that the most important factor was the abrasive grain size. Wear decreases with increasing abrasive grain size. Unal et al. proved this in abrasive tests of different polymers [34, 48-51]. When more asperities encounter the polymer sample, it decreases the effective pressure and potentially leads to lower specific wear rates [35].

Tests with 60-grit abrasives show an increase in wear with increasing filler density from 50% to 75%. Figure 8 shows the average wear in terms of mass loss per pattern and filler density for their 60-grit abrasive counterparts. Sandpapers with large abrasive sizes are assumed to generate a lot of debris, but are unable to retain it between the asperities, causing particles to break off from the contact interface. Both the coefficient of friction and the slope of the friction behavior are likely to decrease further because of the free debris.

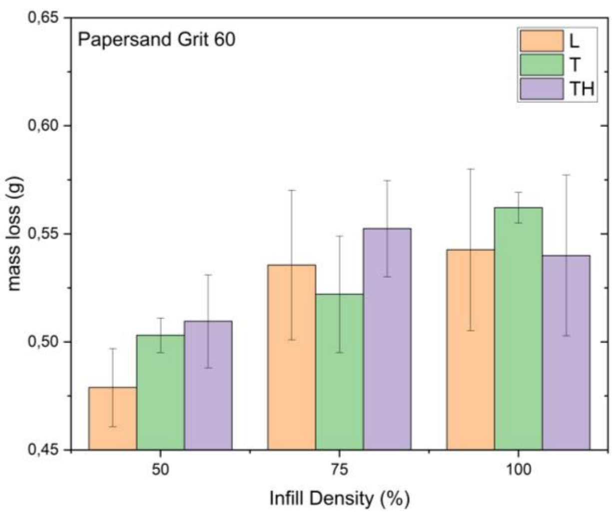

Fig. 8. Mass loss wear versus filler density and filler pattern against 60-grit sandpaper.

An inverse trend was seen in tests using abrasive papers 150-grit and finer. Samples fabricated with a linear infill pattern exhibited a reduction in wear as infill density increased when tested against 150-, 320-, and 600-grit papers (see Fig. 9, 10, and 11).

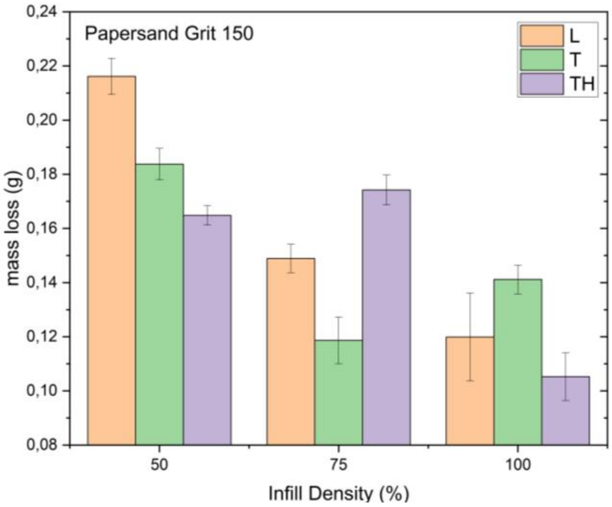

Fig. 9. Mass loss wear versus filler density and filler pattern against 150-grit sandpaper.

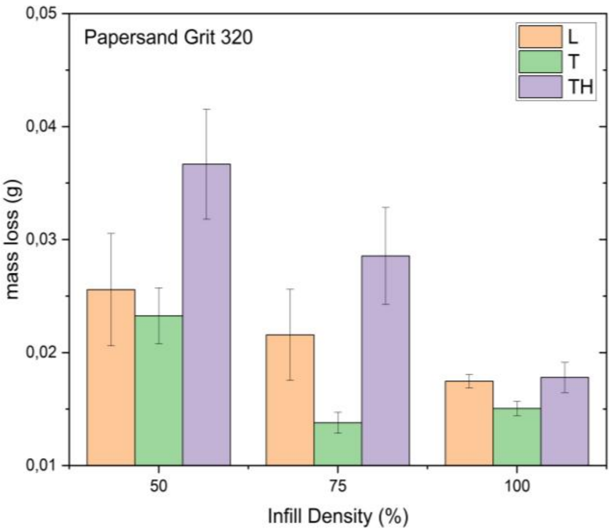

Fig. 10. Mass loss wear versus filler density and filler pattern against 320-grit sandpaper.

Samples with T and TH infill patterns demonstrated a similar wear reduction only in tests with 320-grit paper (see Fig. 9), aligning with the observed low friction and stable tribological behavior for this abrasive condition. Previous studies have suggested that the accumulation of wear debris in the valleys of abrasive papers can influence the specific wear rate of materials [33]. Consequently, wear is further reduced due to the diminished penetration depth of abrasive particles, which is attributed to the filled valleys. Additionally, the entrapment and anchoring of detached particles contribute to a more stable frictional response over repeated sliding cycles, mitigating the abrasive effect [52].

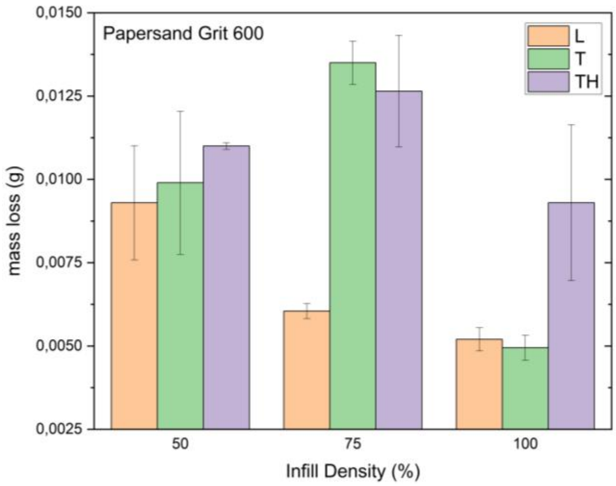

Fig. 11. Mass loss wear versus filler density and filler pattern against 600-grit sandpaper.

Samples with triangular and trihexagonal infill patterns exhibited a general reduction in wear with increasing infill density; However, a consistent decreasing trend was not observed across all grit sizes.

The lowest wear values were recorded in the T/75/150 and T/75/320 tests, but wear increased again at 100% infill density. In contrast, for the T/-/600 tests, wear increased at 75% infill density and decreased again at 100% infill density. Overall, wear was lower at 100% infill density compared to 50% infill density for tests conducted with 150-, 320-, and 600-grit sandpaper. This suggests that as the abrasive particle size decreased, the percentage reduction in wear increased. Specifically, with 150-grit sandpaper, a 24% wear reduction was shown between specimens with 50% and 100% infill density. For 320- and 600-grit abrasives, the reductions reached 33% and 50%, respectively. This shows that as the abrasive grain size decreases, the reduction in wear is greater. This can be attributed to the enhanced ability of denser patterns (100% infill) to generate and sustain a stable transfer film during sliding. Also, transfer films are more readily formed and adhere more effectively to finer abrasives, facilitating smoother contact. In contrast, the presence of internal voids in low-density specimens promotes particle retention at the contact interface, contributing to increased wear and friction fluctuations.

3.3 Wear surfaces

The surfaces of the PLA samples and the wear tracks on the abrasive discs were examined using optical microscopy and digital image processing. Abrasive wear occurs when a hard material removes material from a soft surface, leaving loose or transferred particles in the hard material. Figures 12, 13, 14, and 15 illustrate the representative wear surfaces of the PLA samples after testing. The repeated movement of abrasive particles caused distinct abrasion grooves associated with cutting and ploughing mechanisms. Similar findings were reported by Liu et al. in their abrasive wear tests on polymers [53].

The polymeric samples tested against 60-grit sandpaper exhibited external burrs characterized by faceted segments. The width of these segmented burrs decreased with the reduction in abrasive grain size (see Fig. 12).

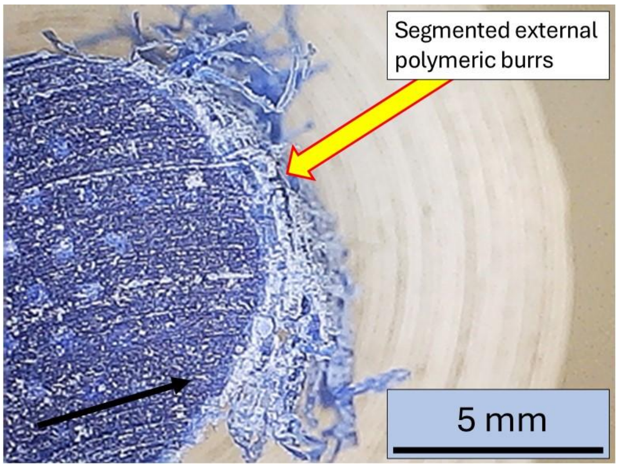

Fig. 12. Worn surface of the polymeric pin from the TH/100/60 test.

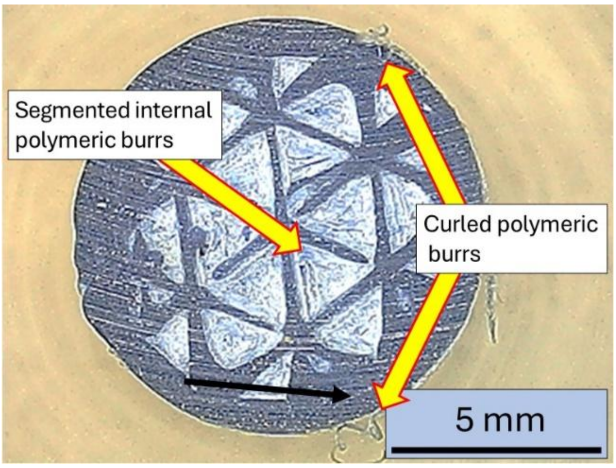

Fig. 13. Worn surface of the polymeric pin from the TH/50/150 test.

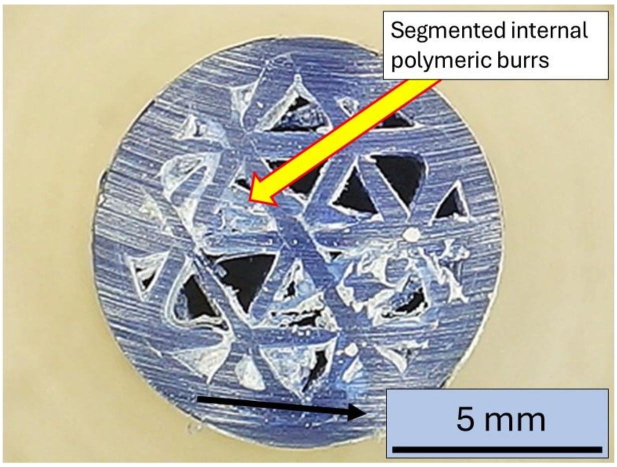

Fig. 14. Worn surface of the polymeric pin from the TH/50/320 test.

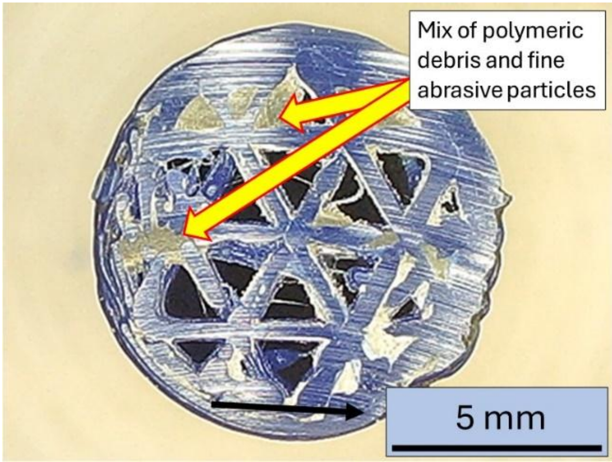

Fig. 15. Worn surface of the polymeric pin from the TH/50/600 test.

These typical burr formations were also observed within the hollow regions of the samples with 50% and 75% infill (see Fig. 13, 14, and 15). The black arrow indicates the sliding direction. A reduction in burr size was observed in 50% and 75% infill samples as the abrasive grain size decreased. As this size decreases, the burrs are more prone to detachment and may be transferred to the contact surface, thereby influencing the frictional behavior. This morphological feature is attributed to plastic deformation and progressive material accumulation. Additionally, surface analysis of the polymeric samples revealed abrasion grooves, microscratches, and plastic deformation. Abrasive particles deeply penetrated the surface, producing microscale ploughing features. The formation of curled polymeric burrs, debris, clumped, and rolled up, was characteristic of the microcutting process (see Fig. 13) [54]. Some elongated particles were likely generated by the detachment of 3D printing filament segments (see Fig. 16 and 17).

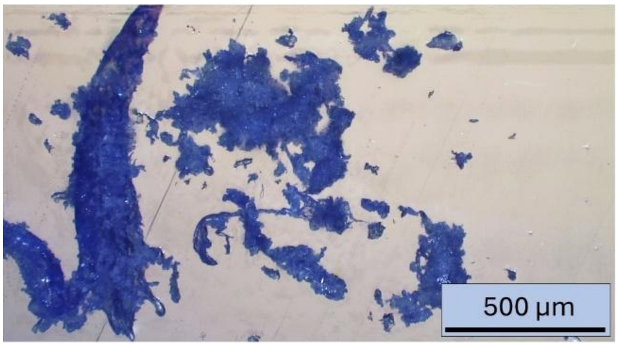

Fig. 16. Typical shapes and sizes of PLA polymer scraps for samples with 50% fill density against 60 grit sandpaper.

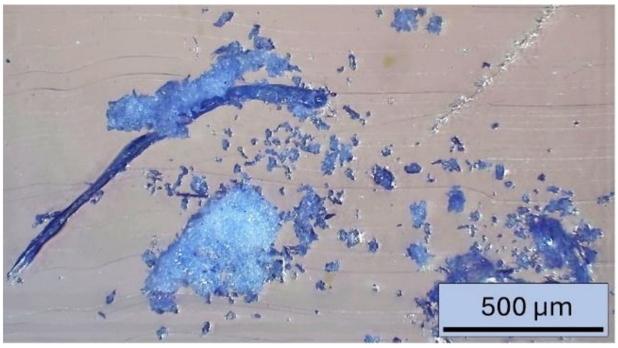

Fig. 17. Typical shapes and sizes of PLA polymer scraps for samples with 50% fill density against 150 grit sandpaper.

A distinct agglomeration of polymeric material and fine abrasive particles was observed only in samples tested with 600-grit sandpaper (see Fig. 15). These polymeric agglomerates exhibited strong adhesion to the PLA surface and were responsible for collecting wear debris, forming so-called “material drag bands” on the abrasive counterpart (see Fig. 18). The observed damage mechanisms, involving combined plastic deformation and complex mechanical stresses during abrasion, are consistent with those reported by Zaghloul et al. [35].

The wear tracks observed on the abrasive paper provided valuable insights into the transferred material and polymeric debris. Figure 18 illustrates the general characteristics of the material that became detached and transferred to the abrasive counterpart. On the abrasive discs, debris and transfer film were identified as particles lodged in the valleys of the abrasive surface, along with clusters of agglomerated particles.

The agglomeration of transferred material results from the accumulation and deformation of particles trapped at the contact interface. The lumps formed through this agglomeration contribute to the formation of a transfer film. Over time, these agglomerates adhered to the abrasive surface, promoting the development of the transfer layer.

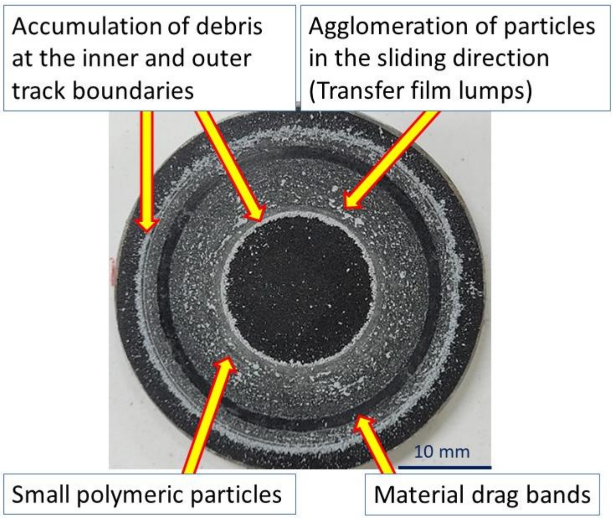

Fig. 18. Typical abrasive wear marks formed on the 600-grit sandpaper during the test.

Particularly, larger lumps of transferred material were observed on the 150-grit abrasive paper. As the abrasive grit size increased from 320 to 600, these agglomerates became nearly imperceptible to the naked eye. When tested with 600-grit abrasive paper, “drag bands” were frequently observed. The drag bands appear as clean wear tracks 1 to 3 mm wide due to the sliding of the mixture of polymeric debris and fine abrasive particles adhering to the polymer sample. The width and position of these drag bands correlated with the agglomerated debris mixtures found on the worn surfaces of polymeric samples tested with 600-grit sandpaper (see Fig. 15). The wear tracks on the abrasive discs showed accumulations of loose particles at both the inner and outer edges of the track. A portion of the detached material was expelled beyond the contact interface, while the remaining fraction adhered to the abrasive surface, forming transferred material. The coarsest abrasive paper (60-grit) generated the highest number of detached debris. The generation of particles with 60-grit sandpaper exceeds the ability to retain them at the interface, expelling them. The continuous release of large amounts of wear debris contributed to a progressive decrease in the coefficient of friction (CoF).

The agglomeration of detached particles is due to thermal softening caused by frictional heating. Compression and crushing at the sliding interface led to the formation of lumps of transferred material on the abrasive surface. Figure 19 shows a section of the wear track with accumulated debris at its edges and clusters of transfer film. The transfer films are composed of agglomerated particles plastically deformed along the sliding direction. Figure 20 provides a detailed view of a transfer film, were individual, non-agglomerated particles can still be seen at the edges of the transferred layer. The surfaces of the abrasive discs exhibited distinct characteristics primarily influenced by abrasive grain size, as shown in Figure 21.

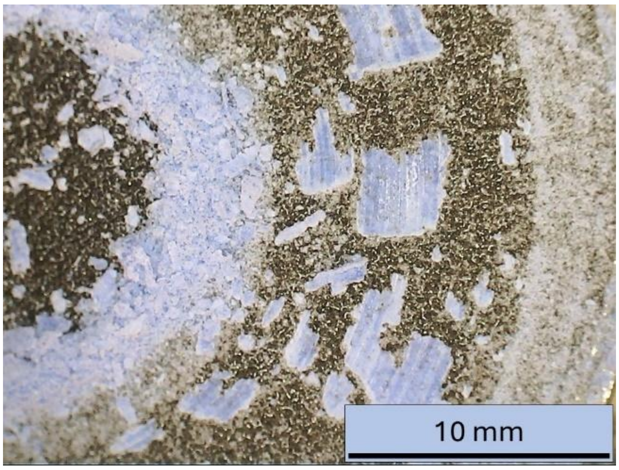

Fig. 19. Lumps of transferred material on 150-grit sandpaper.

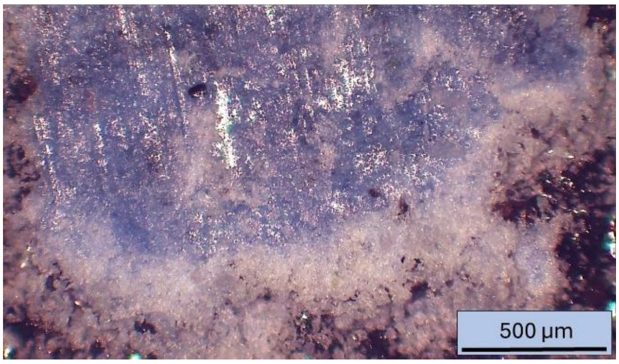

Fig. 20. Typical discontinuous transfer film formed by debris agglomeration on 320-grit sandpaper.

The 60-grit abrasive displayed minimal formation of transferred material lumps, indicating that abrasive wear was the dominant mechanism, with adhesive wear playing a lesser role. In contrast, the 150-grit abrasive paper showed more transferred material lumps.

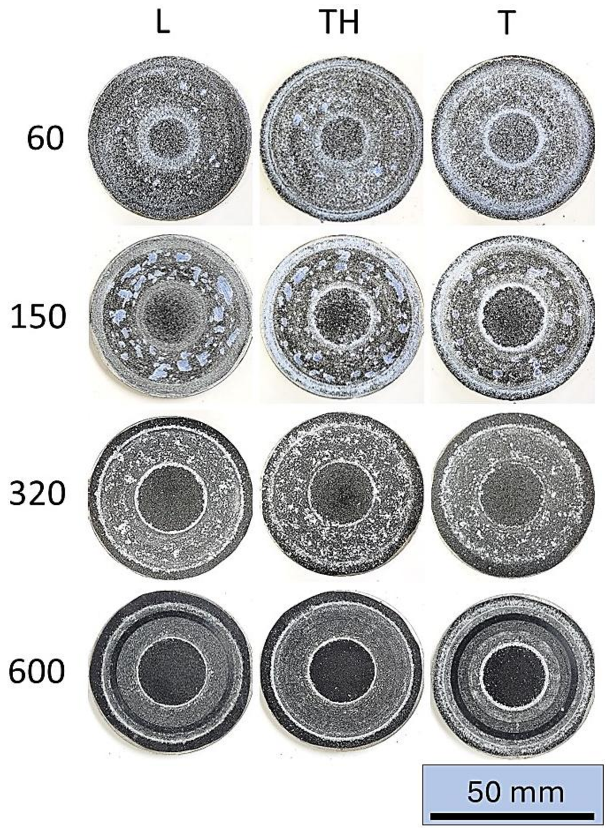

Fig. 21. Abrasive wear tracks for the tests performed with the three filling patterns with 100% infill density.

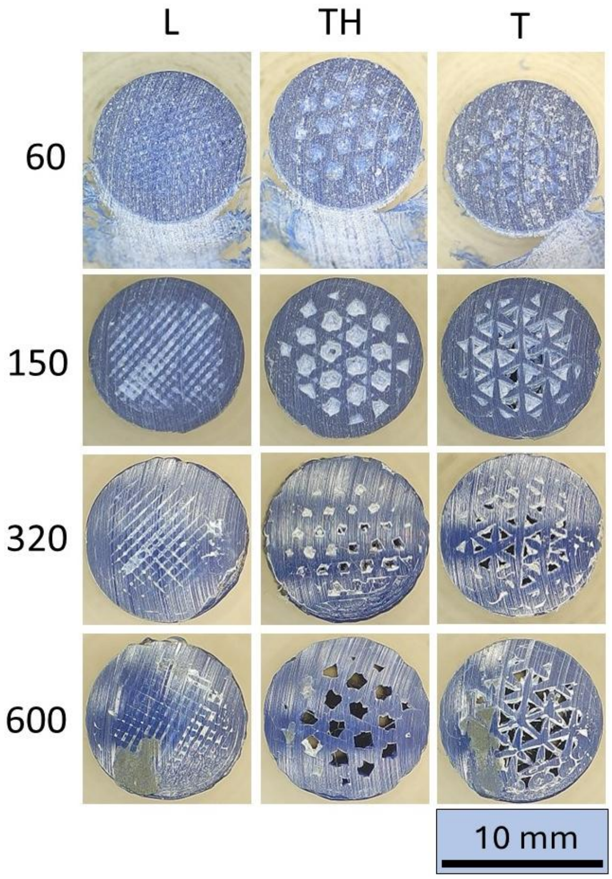

Fig. 22. Typical surfaces of the worn PLA pins for tests performed with the three infill patterns at 75% infill density.

As the abrasive grain size decreased, the count of these lumps progressively diminished, becoming nearly imperceptible with 600-grit sandpaper. When tested against 600-grit abrasive paper, "material drag bands" were observed, suggesting a transition from initial abrasive wear to predominantly adhesive wear. Comparatively, Figure 22 shows typical wear surfaces of PLA pins exhibiting the characteristics described above.

4. CONCLUSION

The abrasive wear behavior of FDM-printed PLA pins was systematically evaluated with three infill patterns (linear, triangular, and trihexagonal) and three infill densities (50%, 75%, and 100%) against four grit sandpapers (60, 150, 320, and 600). Several clear trends were observed in these tests:

1. Frictional behavior and transfer film formation.

- All samples showed a characteristic evolution of the coefficient of friction (CoF), with an initial run-in period followed by stabilization, except for the samples tested against 60-grit sandpaper, which showed a continuous decrease in CoF.
- Pins with higher infill densities (75% and 100%) tended to reach a stable CoF more quickly, due to the rapid buildup of the transfer film at the interface.
- The lowest and most stable CoF (~0.55) was obtained against 320-grit sandpaper, suggesting an optimal balance between asperity contact and debris retention.

2. Wear rate versus abrasive asperity and filler density.

- For medium to fine abrasives (150, 320, and 600-grit), material loss decreased monotonically with increasing infill density; the fully solid pins (100%) showed up to 40% less wear compared to samples with a 50% infill density.
- In contrast, with the coarsest abrasive (60- grit), wear increased with filler density. The rigid, fully dense structure promoted more aggressive cutting with large abrasive particles, overcoming the protection of the transfer film.

3. Role of filler geometry.

- The differences between the linear, triangular, and trihexagonal patterns were slight.
- Overall, the linear and triangular fillers provided slightly better wear resistance, likely because their open channels more easily retained debris, while the denser trihexagonal grid made it difficult for the transfer film to anchor.

4. Surface and Debris Evolution.

- Optical and SEM observations revealed classic abrasive features such as deep grooves, microplowing, and plastic deformation. Coarser grains produced polymeric burrs that decreased in size as the abrasive grain size decreased.
- With 600-grit sandpaper, the agglomeration of debris in the polymeric sample generated clean areas of debris defined as "drag bands" on the abrasive surface. These bands reduced the effective contact area, slightly destabilizing the COF and reducing wear.

The strong dependence of friction and wear on infill density, grain size, and, to a lesser extent, infill pattern, highlights the need to adapt FDM parameters to tribological applications, especially in biomedical implants, automotive seals, or soft tooling components, where predictable, low-wear performance is essential.

Building on the current findings, future investigations will aim to expand the tribological evaluation to include a wider range of infill patterns, such as gyroid and Archimedean spiral patterns, as well as hybrid infill structures. Additionally, multi-stage testing protocols will be introduced, incorporating periodic replacement of the abrasive medium. In this approach, the abrasive paper will be renewed two to four times during testing, allowing assessment under conditions of refreshed abrasivity. Since abrasive particle erosion techniques are also widely employed for post-processing and surface enhancement of 3D-printed components, future research will also explore erosion wear testing on FDM-fabricated PLA materials. The objective is to better understand surface degradation mechanisms and to optimize surface finishing quality in practical engineering applications.

Acknowledgement

The authors wish to thank Gonzalo Ramos and Jeremías Angiano for their generous and committed collaboration in the experimental procedures and the fabrication of test samples. The authors also acknowledge the financial support provided by the National Technological University (UTN) (PID MAUTNHA 7821), and the institutional assistance received from the Institute of Scientific and Technical Research for Defense (CITEDEF).

REFERENCES

[1] S. Sasaki, "Environmentally friendly tribology (Eco-tribology)," *Journal of Mechanical Science and Technology*, vol. 24, no. 1, pp. 67–71, Feb. 2010, doi:10.1007/s12206-009-1154-1.

[2] M. Nosonovsky and B. Bhushan, "Green tribology: Principles, research areas and challenges," *Philosophical Transactions of the Royal Society A: Mathematical, Physical and Engineering Sciences*, vol. 368, no. 1929, pp. 4677–4694, Oct. 2010, doi:10.1098/rsta.2010.0200.

[3] N. A. B. Taib, M. R. Rahman, D. Huda, K. K. Kuok, S. Hamdan, M. K. B. Bakri, M. R. M. B. Julaihi, A. Khan, "A review on poly lactic acid (PLA) as a biodegradable polymer," *Polymer Bulletin*, vol. 80, no. 2, pp. 1179–1213, Mar. 2022, doi:10.1007/s00289-022-04160-y.

[4] U. M. Dilberoglu, B. Gharehpapagh, U. Yaman, and M. Dolen, "The Role of Additive Manufacturing in the Era of Industry 4.0," *Procedia Manuf*, vol. 11, pp. 545–554, Jan. 2017, doi: 10.1016/j.promfg.2017.07.148.

[5] A. Ceci, G. Costanza, G. Savi, & M.E. Tata, "Optimization of the lost PLA production process for the manufacturing of Al-alloy porous structures: Recent developments, macrostructural and microstructural analysis", *International Journal of Lightweight Materials and Manufacture*, vol 7, pp. 662-667, May 2024, doi:10.1016/j.ijlmm.2024.05.007.

[6] M. A. Ali, O. Huseynov, I. Fidan, & F. Vondra, "Lost-PLA Casting Process Development Using Material Extrusion with Low-Weight PLA," *Solid Freeform Fabrication 2023: Proceedings of the 34th Annual International Solid Freeform Fabrication Symposium – An Additive Manufacturing Conf.,* 2023, doi:10.26153/tsw/51025.

[7] M. S. Tunalioglu and B. V. Agca, "Wear and Service Life of 3-D Printed Polymeric Gears," *Polymers (Basel)*, vol. 14, no. 10, May 2022, doi:10.3390/polym14102064.

[8] M. A. Ramadan, "Tribological Investigations of 3D Printed Polymers and Their Applications: A Review," *Journal of Modern Industry and Manufacturing*, Mar. 2022, doi:10.53964/jmim.2022002.

[9] M. R. Derise, M. Rahmat Derise, and A. Zulkharnain, "Effect of Infill Pattern and Density on Tensile Properties of 3D Printed Polylactic acid Parts via Fused Deposition Modeling (FDM)," *IJMME-IJENS*, vol. 20 no. 2, 2020.

[10] M. Lalegani Dezaki and M. K. A. Mohd Ariffin, "The effects of combined infill patterns on mechanical properties in fdm process," *Polymers (Basel)*, vol. 12, no. 12, pp. 1–20, Dec. 2020, doi:10.3390/polym12122792.

[11] J. Ivorra-Martinez, L. Quiles-Carrillo, D. Lascano, S. Ferrandiz, and T. Boronat, "Effect of infill parameters on mechanical properties in additive manufacturing," *Dyna (Spain)*, vol. 95, no. 4, pp. 412–417, Jul. 2020, doi:10.6036/9674.

[12] M. T. Birosz, D. Ledenyák, and M. Andó, "Effect of FDM infill patterns on mechanical properties," *Polymer Testing*, vol. 113, p. 107654, Jun.. 2022, doi:10.1016/j.polymertesting.2022.107654.

[13] B. Aloyaydi, S. Sivasankaran, and A. Mustafa, "Investigation of infill-patterns on mechanical response of 3D printed poly-lactic-acid," *Polymer Testing*, vol. 87, p. 106557, Apr. 2020, doi:10.1016/j.polymertesting.2020.106557.

[14] Y. Li, J. Zheng, C. Sun, and D. Li, "The Transfer Film Effects Induced by 3D Printing Polyether-ether-ketone with Excellent Tribological Properties," *Research Square (Research Square)*, Nov. 2022, doi:10.21203/rs.3.rs-2216558/v1.

[15] D. Hesse, M. Stanko, P. Hohenberg, and M. Stommel, "Investigation of process control influence on tribological properties of FLM-manufactured components," *Journal of Manufacturing and Materials Processing*, vol. 4, no. 2, Jun. 2020, doi:10.3390/jmmp4020037.

[16] M. M. Hanon, R. Marczis, and L. Zsidai, "Impact of 3D-printing structure on the tribological properties of polymers," *Industrial Lubrication and Tribology*, vol. 72, no. 6, pp. 811–818, Aug. 2020, doi:10.1108/ILT-05-2019-0189.

[17] M. M. Hanon and L. Zsidai, "Comprehending the role of process parameters and filament color on the structure and tribological performance of 3D printed PLA," *Journal of Materials Research and*

Technology, vol. 15, pp. 647–660, Nov. 2021, doi:10.1016/j.jmrt.2021.08.061.

[18] P. Zhang, Z. Hu, H. Xie, G. H. Lee, and C. H. Lee, "Friction and wear characteristics of polylactic acid (PLA) for 3D printing under reciprocating sliding condition," *Industrial Lubrication and Tribology*, vol. 72, no. 4, pp. 533–539, Apr. 2020, doi:10.1108/ILT-11-2016-0280.

[19] G. Akıncıoğlu, E. Şirin, and E. Aslan, "Tribological characteristics of ABS structures with different infill densities tested by pin-on-disc," *Proceedings of the Institution of Mechanical Engineers, Part J: Journal of Engineering Tribology*, vol. 237, no. 5, 2023, doi: 10.1177/13506501231153521.

[20] S. Renganathan and S. D, "Effect of fill pattern and printing speed on friction characteristics of FDM printed polylactic acid polymer," *Advances in Materials and Processing Technologies*, vol. 8, no. sup3, pp. 1583–1592, Jul. 2021, doi: 10.1080/2374068X.2021.1948707.

[21] R. Aziz, M. I. U. Haq, and A. Raina, "Effect of surface texturing on friction behaviour of 3D printed polylactic acid (PLA)," *Polymer Testing*, vol. 85, p. 106434, Feb. 2020, doi: 10.1016/j.polymertesting.2020.106434.

[22] I. Portoacă, R. G. Ripeanu, A. Diniță, and M. Tănase, "Optimization of 3D Printing Parameters for Enhanced Surface Quality and Wear Resistance," *Polymers (Basel)*, vol. 15, no. 16, Aug. 2023, doi: 10.3390/polym15163419

[23] V. Mourya, S. P. Bhore, and P. G. Wandale, "Multiobjective optimization of tribological characteristics of 3D printed texture surfaces for ABS and PLA Polymers," *Journal of Thermoplastic Composite Materials*, vol. 37, no. 2, pp. 772–799, Feb. 2024, doi: 10.1177/08927057231185710.

[24] M. A. Ramadan, H. A. Sabour, and E. El-Shenawy, "Tribological Properties of 3D Printed Polymers: PCL, ABS, PLA and Co Polyester," *Tribology in Industry*, vol. 45, no. 1, pp. 161–167, Mar. 2023, doi: 10.24874/ti.1410.11.22.02.

[25] S. Zhiani Hervan, A. Altınkaynak, and Z. Parlar, "Hardness, friction and wear characteristics of 3D-printed PLA polymer," *Proceedings of the Institution of Mechanical Engineers, Part J: Journal of Engineering Tribology*, vol. 235, no. 8, pp. 1590–1598, Aug. 2021, doi: 10.1177/1350650120966407.

[26] B. Istif, "Identification of dry sliding wear behaviour of PLA parts manufactured by fused deposition modelling.," *DÜMF Mühendislik Dergisi*, vol. 12, no. 2, pp. 275–283, Feb. 2021, doi: 10.24012/dumf.855768.

[27] W. Pawlak, W. Wieleba, J. Kluczyński, and L. Śnieżek, "The influence of MoS_2 on the tribological properties of polylactide (PLA) applied in 3D printing technology," *Tribologia*, vol. 289, no. 1, pp. 57–62, Mar. 2020. doi: 10.5604/01.3001.0014.0848.

[28] V. K. Tiwary, A.P, A.S. Deshpande, N Rangaswamy, "Surface enhancement of FDM patterns to be used in rapid investment casting for making medical implants," *Rapid Prototyping Journal*, vol. 25, no. 5, pp. 904-914, Jun. 2019, doi:10.1108/RPJ-07-2018-0176.

[29] E. Ol'khovik, "Study of abrasive resistance of foundries models obtained with use of additive technology," *IOP Conference Series: Earth and Environmental Science, IOP Publishing*, vol. 87, no. 9, p. 092019, Oct. 2017, doi:10.1088/1755-1315/87/9/092019.

[30] M. Kujawa & A. Ptak, "The Experimental Comparison of Abrasion Resistance of Extruded and 3D Printed Plastics," *Materials*, vol. 18, no. 7, Apr. 2025, doi: 10.3390/ma18071592.

[31] M. Vaziri, R. T. Spurr, and F. H. Stott, "An investigation of the wear of polymeric materials," *Wear*, vol. 122, no. 3, pp. 329-342, Mar. 1988, doi: 10.1016/0043-1648(88)90018-X.

[32] J. M. Thorp, "Abrasive wear of some commercial polymers," *Tribology International,* vol. 15, no. 2, pp. 59-68, Apr. 1982, doi: 10.1016/0301-679X(82)90054-8.

[33] M. M. Y. Zaghloul, K. Steel, M. Veidt, D. Martin, M. Firouzi, and M. T. Heitzmann, "Influence of Counter-Face Grit Size and Lubricant on the Abrasive Wear Behaviour of Thermoplastic Polymers Reinforced with Glass Fibres," *Tribology Letters*, vol. 71, no. 3, Aug. 2023, doi: 10.1007/s11249-023-01774-9.

[34] H. Unal, U. Sen, and A. Mimaroglu, "Abrasive wear behaviour of polymeric materials," *Materials & Design (1980-2015)*, vol. 26, no. 8, pp. 705–710, Dec. 2004, doi: 10.1016/j.matdes.2004.09.004.

[35] M. M. Y. Zaghloul, K. Steel, M. Veidt, and M. T. Heitzmann, "Assessment of the tribological performance of glass fibre reinforced polyamide 6 under harsh abrasive environments," *Tribology International*, vol. 191, p. 109059, Nov. 2023, doi: 10.1016/j.triboint.2023.109059.

[36] M. A. Zainal, K. I. Ismail, and T. C. Yap, "Tribological Properties of PLA 3D Printed at Different Extrusion Temperature," *Journal of Physics Conference Series*, vol. 2542, no. 1, p. 012001, Jul. 2023, doi:10.1088/1742-6596/2542/1/012001.

[37] P. Yaman, O. Ekşi, S. S. Karabeyoğlu, and K. Feratoğlu, "Effect of build orientation on tribological and flexural properties of FDM-printed composite PLA parts," *Journal of Reinforced Plastics and Composites*, vol. 43, no. 1–2, pp. 97–110, Jan. 2024, doi: 10.1177/07316844231157790.

[38] D. Frunzaverde et al., "The Influence of the Layer Height and the Filament Color on the Dimensional Accuracy and the Tensile Strength of FDM-Printed PLA Specimens," *Polymers (Basel)*, vol. 15, no. 10, May 2023, doi: 10.3390/polym15102377.

[39] ASTM G99-17, "Standard Test Method for Wear Testing with a Pin-on- Disk Apparatus," American Society for Testing and Materials (ASTM) International, West Conshohocken.2017,

[40] L. Palaniandy, K. I. Ismail, and T. C. Yap, "Tribological Behaviour of 3D printed Polylactic Acid (PLA) Sliding Against Steel at Different Sliding Speed," *Journal of Physics Conference Series*, vol. 2542, no. 1, p. 012003, Jul. 2023. doi: 10.1088/1742-6596/2542/1/012003.

[41] S. Guicciardi, C. Melandri, F. Lucchini, and G. De Portu, "On data dispersion in pin-on-disk wear tests," *Wear*, vol. 252, no. 11–12, pp. 1001–1006, Jul.2002. doi:10.1016/S0043-1648(02)00066-2.

[42] J. Sedlak, L. Spisak, D. Hrusecka, E. Jurickova, L. Hrbackova, and Z. Joska, "Analysis of test plastic samples printed by the additive method fused filament fabrication," *MM Science Journal*, vol. 2021, no. 1, pp. 4283–4290, Mar. 2021, doi: 10.17973/MMSJ.2021_03_2020075.

[43] C. P. Valerga, M. Batista, R. Puyana, A. Sambruno, C. Wendt, and M. Marcos, "Preliminary study of PLA wire colour effects on geometric characteristics of parts manufactured by FDM," *Procedia Manufacturing*, vol. 13, pp. 924–931, Jan. 2017, doi: 10.1016/j.promfg.2017.09.161.

[44] M. N. M. Norani, M. I. H. C Abdullah, M. F. B Abdollah, H. Amiruddin, F. R. Ramli, and N. Tamaldin, "Tribological analysis of a 3D-printed internal triangular flip ABS pin during running-in stage,"*Jurnal Tribologi*, vol 27, pp. 42-56, 2020.

[45] E. G. Ertane, A. Dorner-Reisel, O. Baran, T. Welzel, V. Matner, and S. Svoboda, "Processing and Wear Behaviour of 3D Printed PLA Reinforced with Biogenic Carbon," *Advances in Tribology*, vol. 2018, pp. 1-11, Aug. 2018, doi:10.1155/2018/1763182.

[46] V. A. Bely, V. A., Sviridenok, A. I., & Petrokovets, M. I. Friction and wear in polymer-based materials. Elsevier, Pergamon Press 2013.

[47] D. Fouly, A. K. Assaifan, I. A. Alnaser, O. A. Hussein, and H. S. Abdo, "Evaluating the Mechanical and Tribological Properties of 3D Printed Polylactic-Acid (PLA) Green-Composite for Artificial Implant: Hip Joint Case Study," *Polymers (Basel)*, vol. 14, no. 23, Dec. 2022, doi: 10.3390/polym14235299.

[48] A. Mimaroglu, U. Sen, and H. Unal, "Abrasive wear volume maps for PA6 and PA6 composites under dry working condition," *Applied Composite Materials*, vol. 15, no. 1, pp. 13–25, Jan. 2008, doi: 10.1007/s10443-008-9054-6.

[49] H. Muhandes, Á. Kalácska, L. Székely, R. Keresztes, and G. Kalácska, "Abrasive sensitivity of engineering polymers and a bio-composite under different abrasive conditions," *Materials*, vol. 13, no. 22, pp. 1–27, Nov. 2020, doi: 10.3390/ma13225239.

[50] S. Krupesh, R. Suresh, B. M. Rudresh, and K. Ajaykumar, "Effect of abrasive grit grade on the abrasion wear behaviour of long banana-jute fibers reinforced hybrid epoxy composites," *Mater Res Express*, vol. 10, no. 12, Dec. 2023, doi: 10.1088/2053-1591/ad1126.

[51] B. V. Lingesh, B. N. Ravikumar, and B. M. Rudresh, "Investigation on the Effect of Grit size on Two Body Abrasive Wear Behavior of Polyamide66/Polypropylene (PA66/PP) blends," *in Materials Today: Proceedings, Elsevier Ltd*, vol. 5, no. 1, pp. 2444–2452, Jan. 2018, doi: 10.1016/j.matpr.2017.11.024.

[52] S. Kumar and K. Panneerselvam, "Two-body Abrasive Wear Behavior of Nylon 6 and Glass Fiber Reinforced (GFR) Nylon 6 Composite," *Procedia Technology*, vol. 25, pp. 1129–1136, 2016, doi: 10.1016/j.protcy.2016.08.228.

[53] C. Liu, L. Ren, R. D. Arnell, and J. Tong, "Abrasive wear behavior of particle reinforced ultrahigh molecular weight polyethylene composites," *Wear*, vol. 225-229, pp. 199–224, Apr. 1999, doi:10.1016/S0043-1648(99)00011-3.

[54] E. Tan, "Experimentally Assessing the Wear Characteristics of 3D-Printed PLA and Tough PLA Materials Based on Fused Deposition Modeling," *Gazi Journal of Engineering Sciences*, vol. 9, no. 2, pp. 213–226, Aug. 2023, doi: 10.30855/gmbd.0705065.